Supporting Information

Fabrication of nitrogen-enriched carbon dots with green fluorescence for enzyme-free detection of uric acid

Fengxiang Wang [a]*, Xinyue Chai[a], Xinyang Fu[a], Guojiang Mao[c], Hua Wang[a,b]*

[a]College of Chemistry and Chemical Engineering, Qufu Normal University, Qufu, Shandong, 273165, P. R. China.
[b]Huzhou Key Laboratory of Medical and Environmental Applications Technologies, School of Life Sciences, Huzhou University, Huzhou City, Zhejiang Province 313000, PR, China.
[c]Henan Key Laboratory of Organic Functional Molecule and Drug Innovation, School of Chemistry and Chemical Engineering, Henan Normal University, Xinxiang, Henan, 453007, P. R. China.

Table of Contents

Experimental Section

Chemicals and materials

Uric acid (UA), glucose, lactose, bovine serum albumin (BSA), ascorbic acid (AA), dopamine (DA), lactic acid (LA), urea, citric acid (CA), glutathione (GSH), cysteine (Cys), glycine (Gly), histidine (His), phenylalanine (Phe), leucine (Leu), glutamic acid (Glu), tyrosine (Tyr), KSCN, creatinine (Cre), oxalic acid (OA), Na_2HPO_4, NaH_2PO_4, catechol, resorcinol and hydroquinone were obtained from Aladdin Reagent Co. (Shanghai, China). Anhydrous inorganic salts, ethylenediamine (EDA) and other chemical reagent in this paper were purchased from Beijing Chemical Reagent Co., Ltd (Beijing, China). And all the chemicals used were analytical grade and used directly without further purification. Ultra-pure water was supplied from an Ultra-pure water system (Pall, USA).

Characterization

The fluorescence measurements were carried out with a FluoroMax-4 fluorescence spectrophotometer (Horiba, Japan). Fluorescence decay curves were carried out with the FLS 1000-stm (Edinburgh Instruments, UK). The UV-vis spectrum was recorded at room temperature on a UV-3600 spectrophotometer (Shimadzu, Japan). Fourier transform infrared spectroscopy (FT-IR) were tested on a Nicolet IS-10 spectrometer (Thermo-Fisher, America). Transmission electron microscopy (TEM, JEM-2100PLUS, Japan) imaging operated at 100 kV and X-Ray photoelectron spectroscopy (XPS, Thermo-Fisher ESCALAB 250, America) was employed to characterize the morphological and chemistry structures of materials. The photographs of corresponding reaction products were obtained under UV light at exciting wavelength of 365 nm.

Collection of saliva samples

Artificial saliva was prepared by a facile method based on reported work [1]. Briefly, an appropriate amount of NaCl, $CaCl_2$, KCl, NH_4Cl, citric acid and glucose were added into 25 mL Ultra-pure water to be dissolved ultrasonically, and adjusting the pH to 6.7 with NaOH solution. The concentration of each substance the artificial saliva is 5 mM NaCl, 1 mM $CaCl_2$, 15 mM KCl, 1 mM citric acid, 100 μM glucose, and 4 mM NH_4Cl.

Samples of human saliva were collected from healthy laboratory coworkers using "passive drool method" [2, 3], Samples of human saliva are usually collected in the morning after an 8-h fasting since saliva production is increased after eating using the following procedure:

a) Brush teeth the night before the collection.

b) Avoid smoking, food and fluid ingestion or chewing gum for at least 30 min before collection.

Calculation of quantum yields (QY) of NCDs

QY of the NCDs was measured by comparing the integrated fluorescence intensities and absorbance values against the reference quinine sulfate with the QY of 54%, according to the measurement method reported elsewhere [4]. The QY of NCDs was thus calculated by the following equation:

$$\Phi_X = \Phi_{ST}(m_X / m_{ST})(\eta^2{}_X / \eta^2{}_{ST})$$

$$m_X = F_X / A_X$$

$$m_{ST} = F_{ST} / A_{ST}$$

Here, the ST and X represent the standard reference and the sample to be tested, respectively. Φ and F separately refer to the quantum yield and the fluorescence intensity. The m refer to the slope value obtained by plotting the integrated fluorescence intensity and absorption intensity in the slope method. The η and A are the refractive index and the UV-vis absorption intensity.

Stern-Volmer equation

The Stern-Volmer equations (1) and (2) correspond to dynamic quenching type (collisional deactivation) and static quenching type (complexation).

$$F_0/F = \tau_0/\tau = 1 + k_q \tau_0 [Q] \quad (1)$$

$$F_0/F = 1 + K_{SV}[Q] \quad (2)$$

Where F_0 and F are the fluorescence intensities in the absence and presence of the quenchers, respectively, and τ_0 and τ are the lifetimes of the fluorescent materials in the absence and presence of the quenchers, respectively. [Q] and k_q are the quencher concentration and the constant of dynamic (collisional) quenching, respectively. K_{SV} is the constant of static quenching in Eq. (2). In particular, the lifetime is unchanged for static quenching in the absence and presence of quenchers, where the value of τ_0/τ is equal to 1.

Chart Section

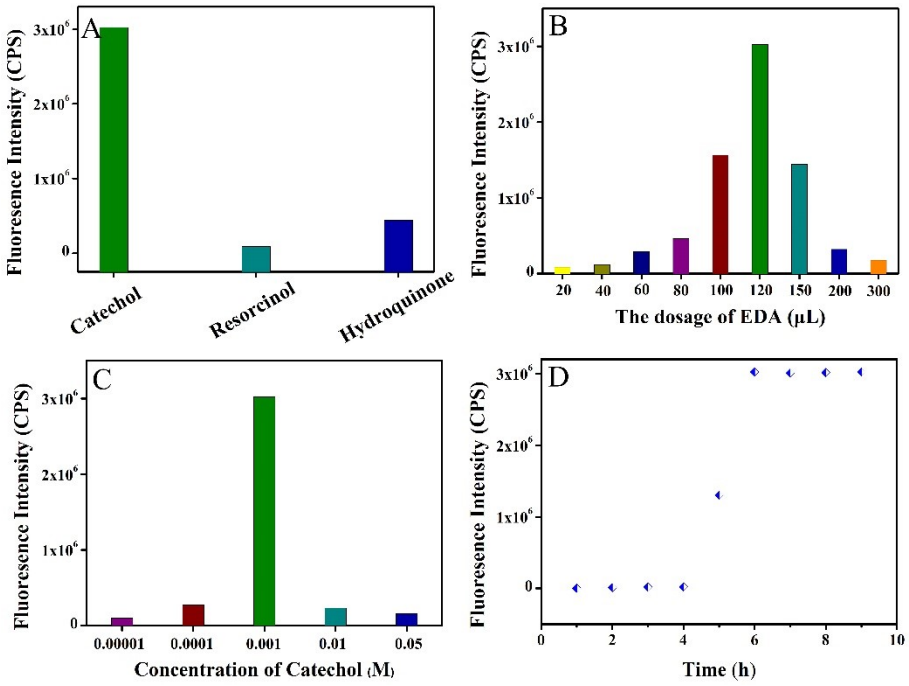

Fig. S1 The effect of reaction conditions on FL properties of NCDs: (A) different isomers, (B) the dosage of EDA, (C) concentration of catechol, (D) reaction time.

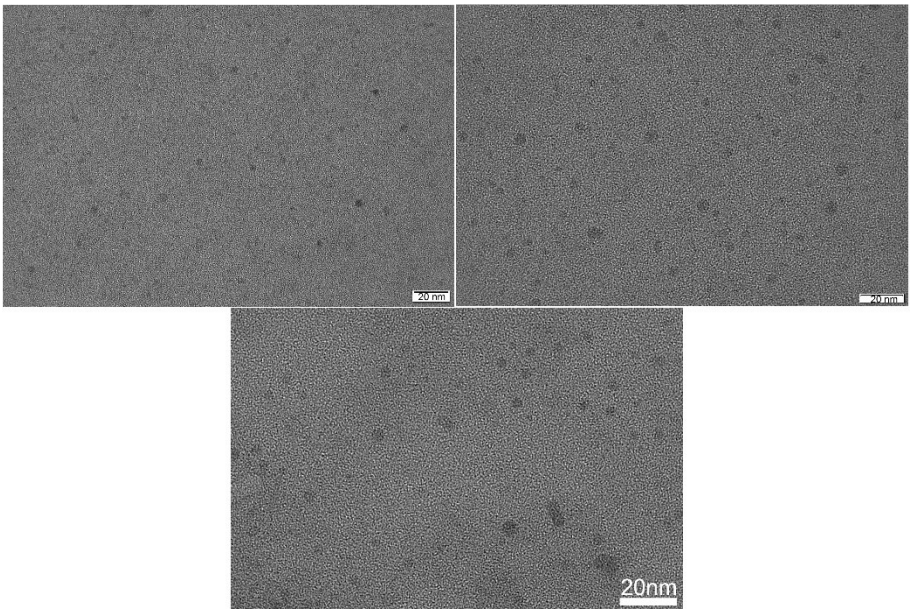

Fig. S2 TEM images of NCDs.

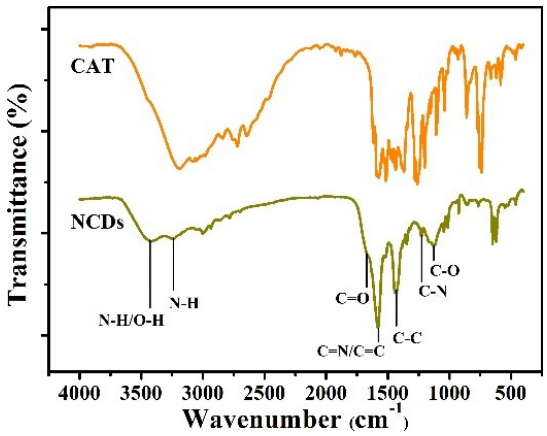

Fig. S3 FT-IR spectra of the NCDs and CAT.

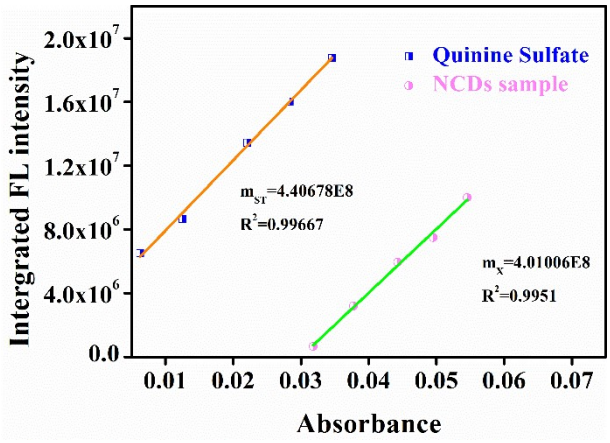

Fig. S**4** Integrated fluorescence intensity versus absorbance plot of NCDs and quinine sulphate.

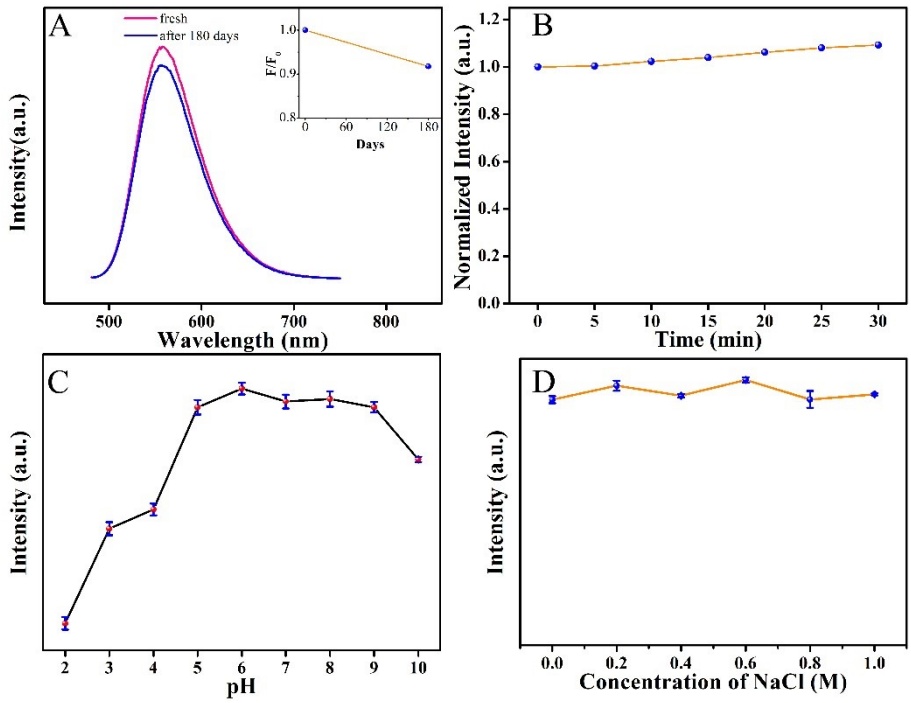

Fig. S5 FL intensity variations of the NCDs as a function of (A) storage time, (B) UV exposure (30 mins), the effect of pH (C) (2.0, 3.0,4.0, 5.0, 6.0, 7.0, 8.0, 9.0 and 10.0) and ion strengths in NaCl (D) (0.0, 0.2, 0.4, 0.6, 0.8 and 1.0 M) on the FL intensity at 555 nm (Ex 412 nm).

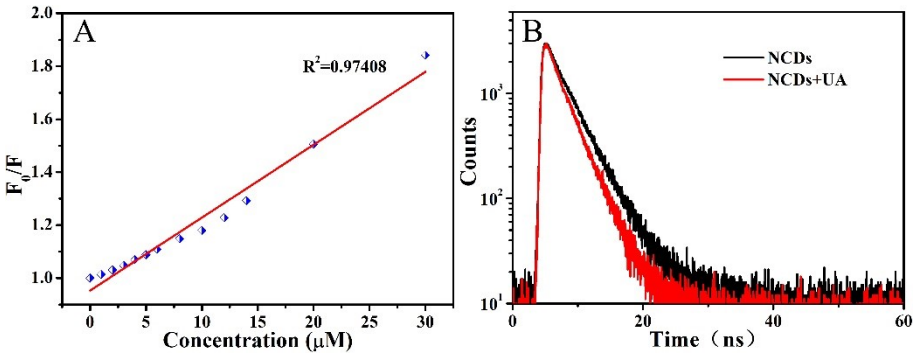

Fig. S6 (A) Stern-Volmer plots describes the dependency of the FL intensities on the UA concentration over the range of 0-30 μM, (B) FL decay curves of NCDs in absence and presence of UA.

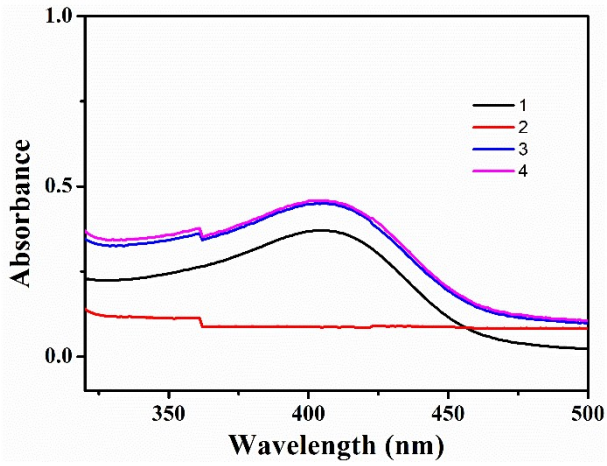

Fig. S7 (A) UV-vis absorption spectra. (1 - NCDs, 2 - 30 μM UA, 3 - NCDs+30 μM UA, 4 - mathematical addition of curves 1 and 2)

Table S1 XPS analysis results of NCDs

Element	Atomic percent (%)
C	64.69
N	23.49
O	11.82

Table S2 Comparison of fluorescent analytical methods for UA detection

Material	Enzyme or Enzyme-free	Indirect or Direct	Linear range (μM)	LoD (μM)	Ref.
CdS quantum dots	Enzyme	Indirect	125-1000	125	[5]
NaYF4 nanoparticles	Enzyme	Indirect	10-1000	2.86	[6]
CdTe nanoparticles	Enzyme	Indirect	25-250	0.01	[7]
S, N co-doped carbon dots	Enzyme	Indirect	0.08-10 μM and 10-50 μM	0.07	[8]
Gold nanoclusters	Enzyme	Indirect	5-100	1.7	[9]
CDs & MnO_2 nanosheets	Enzyme-free	Indirect	0.1-200	0.045	[10]
CDs	Enzyme-free	Direct	0.1-100	0.05	[11]
Nitrogen, Cobalt Co-doped CDs	Enzyme	Indirect	0.01-300	0.0034	[12]
Gold/silver nanoclusters	Enzyme	Indirect	0-90	5.1	[13]
Nitrogen-doped carbon nanodots	Enzyme-free	Indirect	0.0075-1	0.0023	[14]
N-CDs & OPD	Enzyme	Indirect	0.5-150	0.06	[15]
Eu-MOF nanofiber	Enzyme-free	Direct	0-200	0.6	[16]
Carbon quantum dots	Enzyme-free	Direct	1-17	0.94	[17]
Carbon dots	Enzyme	Indirect	0-56	0.49	[18]
Sulfur quantum dots	Enzyme	Indirect	1-10	0.56	[19]
NCDs	Enzyme-free	direct	0-30	0.22	this work

Table S3 Detection of UA in artificial saliva and human saliva samples by this proposed method

Samples	Cumulative added/μM	Found /μM	Recovery (%)	RSD (%) (n=5)
artificial saliva	0	-	-	-
	8	8.39	104.8	2.43
	15	15.49	103.3	1.99
sample 1	0	7.53	-	3.01
	5	12.78	102.0	2.72
	10	17.91	102.0	2.57
sample 2	0	10.58	-	2.32
	5	15.95	102.3	2.06
	10	21.19	102.9	2.12

*Sample 1 and 2 refer to human saliva sample 1 and human saliva sample 2, respectively.

References:

1. Azeredo, N.F.B., et al., *Uric acid electrochemical sensing in biofluids based on Ni/Zn hydroxide nanocatalyst.* Microchimica Acta, 2020. **187**(7): p. 379.
2. Kim, J., et al., *Non-invasive mouthguard biosensor for continuous salivary monitoring of metabolites.* Analyst, 2014. **139**(7): p. 1632-1636.
3. Vernerová, A., et al., *Non-invasive determination of uric acid in human saliva in the diagnosis of serious disorders %J Clinical Chemistry and Laboratory Medicine (CCLM).* Clinical Chemistry and Laboratory Medicine, 2021. **59**(5): p. 797-812.
4. Zhou, J., et al., *An Electrochemical Avenue to Blue Luminescent Nanocrystals from Multiwalled Carbon Nanotubes (MWCNTs).* Journal of the American Chemical Society, 2007.

129(4): p. 744-745.

5. Azmi, N.E., et al., *A simple and sensitive fluorescence based biosensor for the determination of uric acid using H2O2-sensitive quantum dots/dual enzymes.* Biosensors and Bioelectronics, 2015. **67**: p. 129-133.
6. Sheng, Y., et al., *Silver nanoclusters-catalyzed luminol chemiluminescence for hydrogen peroxide and uric acid detection.* Talanta, 2017. **166**: p. 268-274.
7. Jin, D., et al., *Quantitative determination of uric acid using CdTe nanoparticles as fluorescence probes.* Biosensors and Bioelectronics, 2016. **77**: p. 359-365.
8. Wang, H., et al., *High fluorescence S, N co-doped carbon dots as an ultra-sensitive fluorescent probe for the determination of uric acid.* Talanta, 2016. **155**: p. 62-69.
9. Liu, Y., et al., *Gold nanoclusters as switch-off fluorescent probe for detection of uric acid based on the inner filter effect of hydrogen peroxide-mediated enlargement of gold nanoparticles.* Biosensors and Bioelectronics, 2017. **91**: p. 734-740.
10. Yang, J., et al., *A facile fluorescence assay for rapid and sensitive detection of uric acid based on carbon dots and MnO2 nanosheets.* New Journal of Chemistry, 2018. **42**(18): p. 15121-15126.
11. Zhao, C., et al., *Green synthesis of carbon dots from pork and application as nanosensors for uric acid detection.* Spectrochimica Acta Part A: Molecular and Biomolecular Spectroscopy, 2018. **190**: p. 360-367.
12. Huang, S., et al., *Nitrogen, Cobalt Co-doped Fluorescent Magnetic Carbon Dots as Ratiometric Fluorescent Probes for Cholesterol and Uric Acid in Human Blood Serum.* ACS Omega, 2019. **4**(5): p. 9333-9342.
13. Wang, X.-y., et al., *A novel ratiometric fluorescent probe for the detection of uric acid in human blood based on H2O2-mediated fluorescence quenching of gold/silver nanoclusters.* Talanta, 2019. **191**: p. 46-53.
14. Wu, W.-C., et al., *Nitrogen-doped carbon nanodots prepared from polyethylenimine for fluorometric determination of salivary uric acid.* Microchimica Acta, 2019. **186**(3): p. 166.
15. Li, F., et al., *A highly sensitive dual-read assay using nitrogen-doped carbon dots for the quantitation of uric acid in human serum and urine samples.* Microchimica Acta, 2021. **188**(9): p. 311.
16. Zheng, Q., et al., *An enzyme-free fluorescent sensing platform for the detection of uric acid in human urine.* Journal of Luminescence, 2021. **236**: p. 118076.
17. Li, G.-W., et al., *Carbon quantum dots with green fluorescence as a probe for detecting uric acid.* Chemical Papers, 2022.
18. Pang, X., et al., *Non-doped and non-modified carbon dots with high quantum yield for the chemosensing of uric acid and living cell imaging.* Analytica Chimica Acta, 2022. **1199**: p. 339571.
19. Rong, S., et al., *Novel and facile synthesis of heparin sulfur quantum dots via oxygen acceleration for ratiometric sensing of uric acid in human serum.* Sensors and Actuators B: Chemical, 2022. **353**: p. 131146.